Int. J. Electrochem. Sci., 8 **(2013)** 11734 - 11751

International Journal of
ELECTROCHEMICAL
SCIENCE
www.electrochemsci.org

Comparison of Electrochemical Noise Method with the Conventional Electrochemical Techniques for Investigation of the Pitting Corrosion on Al Alloys AA6061 and AA5052

M. Shahidi[1,*], *H. Tajabadipour*[2], *H. Ganjalikhan Hakemi*[1], *M.R. Gholamhosseinzadeh*[1]

[1] Department of Chemistry, Kerman Branch, Islamic Azad University, Kerman, Iran.
[2] Department of Chemistry, Marvdasht Branch, Islamic Azad University, Marvdasht, Iran.
[*]E-mail: shahidi@iauk.ac.ir

Received: 2 July 2013 / *Accepted:* 4 August 2013 / *Published:* 10 September 2013

The corrosion of aluminum alloys AA6061 and AA5052 in 3.5% NaCl solution and when this solution is doped with each of acetate, chromate and citrate at 0.002 M have been investigated by potentiodynamic polarization, electrochemical impedance spectroscopy (EIS) and electrochemical noise (EN) techniques. The goal of this paper is to compare the results obtained from polarization and EIS techniques with those acquired from the wavelet analysis of EN measurements on the pitting corrosion of Al alloys. The study of standard deviation of partial signal (SDPS) plots arising from wavelet analysis provides a convenient way of comparing the pit size and pit density in several corroding systems. The SDPS plots prove the inhibition action of acetate and chromate both on the pit size and the pit density of Al alloys. According to the SDPS plots it is possible to recognize the inhibition effect of citrate on the pit size and its acceleration effect on the pit density. Based on the calculation of the total amount of noise charges arising from all of partial signals it is possible to obtain the inhibition efficiency (IE) of an inhibitor. The IE values show a reasonable agreement with those obtained from potentiodynamic polarization and EIS methods. Therefore, the wavelet analysis of EN data seems as an alternative tool to overcome the limitations of the polarization and EIS techniques in the pitting corrosion monitoring applications.

Keywords: Electrochemical noise; Wavelet analysis; Standard deviation of partial signal; Inhibition efficiency.

1. INTRODUCTION

Electrochemical noise (EN) technique is one of the most promising methods for monitoring and studying of corrosion processes [1-15]. EN is defined as the fluctuations of potential or current originating from the localized events in a corrosion process. EN measurements can be performed in freely corroding systems without the external application of electrical signals, so that the natural evolution of corrosion processes is assured. The standard method use to measure EN is a three electrode arrangement in which two nominally identical working electrodes (WE) are connected via a zero-resistance ammeter (ZRA) monitoring the coupling current between the electrodes [1]. While the electrochemical noise measurement is simple, the electrochemical noise analysis remains difficult. Wavelet transform (WT) is a mathematical tool that has gained popularity [3-15]. WT may be regarded as a variant of Fourier transform in which the continuous sine waves used in the Fourier transform are replaced by transients with a finite duration, known as wavelets. WT approach, unlike Fourier transform can retain time domain information and also it can analyze non-stationary signals without the requirement for pre-processing methods [8].

The time record is transformed to the wavelet coefficients which measure the similarity between the wavelet function and different segments of signal. Each set of coefficients, $d_1, d_2, \ldots, d_J$ and s_J is called a crystal.

The scale range of each crystal is given by the equation [3]:

$$(I_1, I_2) = \left(2^j \Delta t \ , \ 2^{j-1} \Delta t \right) \tag{1}$$

where Δt is the sampling interval ($\Delta t = 1/f_s$, f_s is sampling frequency) and j is the number of the crystal. Table 1 shows the scale range of the case in which $J = 8$ and $f_s = 4Hz$.

Table 1. The scale range for $J = 8$ and $f_s = 4Hz$.

Crystal name	Scale range/s
d1	0.25 – 0.5
d2	0.5 - 1
d3	1 - 2
d4	2 – 4
d5	4 – 8
d6	8 – 16
d7	16 – 32
d8	32 – 64

The original signal can be reconstructed by adding together the contributing wavelets weighted by their corresponding coefficients [4]. This process is known as inverse WT, and it produces one smooth signal, PSs_J, and J detail signals, PSd_j. Each of these $J+1$ signals is called a partial signal (PS) [4, 13]. Each PS is a signal which resembles the fluctuations of the original signal at a particular interval of scale range. For example $PSd5$ represents all fluctuations of the original signal between $4-8$ s, if the sampling frequency is equal to 4 Hz (Table 1). The unit of PS is the same as that of the EN signal.

One important way of representing the results of wavelet transform is the standard deviation of partial signal (SDPS) [13]. SDPS can indicate the variations in the intensity of the PS about its mean, which could be an indication of the intensity of electrochemical activity on the surface of the electrodes within a particular frequency interval. The plot of the SDPS values vs. their corresponding crystal name is called SDPS plot and it has the potential utility for analyzing EN records. The SDPS plot can detect the predominant transients of each signal by the position of the maximum peak. The SDPS plots also can categorize several EN signals according to the intensity of various frequencies they represent.

Aluminum and aluminum alloys resistance to corrosion is attributed to the rapidly formed stable oxide film. Although the oxide film is a good electrical insulator, it is susceptible to pitting corrosion in the presence of aggressive anions, such as chloride [2, 7, 9]. Pitting corrosion occurrence can be minimized by the use of inhibitors. It is possible to classify the anions according to their action upon aluminum in three classes [16]: (1) anions not forming complexes: (a) non-oxidizing, e.g. benzoate, phosphate, sulfate and acetate: corrosion in these is inhibited over the neutral range of pH in solutions of these ions, and (b) oxidizing, e.g. chromate and nitrate: corrosion is inhibited over a wider range of pH than for solutions of 1-a anions, (2) anions forming soluble complexes with aluminum, e.g. citrate and tartrate: more corrosion occurs in solutions of this type than with anions of group 1, and (3) anions not forming soluble complexes and causing corrosion of aluminum in solutions of neutral pH, e.g. chloride.

The effect of inhibitors on the corrosion of Al alloys has been studied by conventional techniques such as polarization and electrochemical impedance spectroscopy (EIS) testing [17, 18]. Electrochemical noise technique as the only truly noninvasive electrochemical method can provide more information of localized corrosion than the conventional techniques, especially when the wavelet transform is applied to analyze the EN data.

In this work the behavior of alloys AA6061 and AA5052 in sodium chloride solution is compared with their behavior when this solution is doped with one of the anions of acetate, chromate or citrate at 0.002M by using potentiodynamic polarization, EIS and EN techniques. In the EN method the SDPS plots arising from WT have been employed to interpret the current noise data.

2. EXPERIMENTAL

2.1. Specimens preparation

Two Al alloys, AA6061 (rod type) and AA5052 (plate type), have been employed in this work whose chemical composition are given in Table 2.

Table 2. Chemical composition of Al alloys.

Alloy type	Mg	Fe	Si	Cr	Cu	Al
AA6061	0.33	0.49	0.28	-	0.13	Balance
AA5052	1.85	0.40	0.22	0.19	-	Balance

Before performing experiments, the specimens were connected to a copper wire at one end sealed using resin, with the other end that exposed a working surface area of 1 cm^2 to the electrolyte. Then the working surface was polished by wet abrasive papers through 600-2500-grade, washed with distilled water, degreased with ethanol, finally dried in air. The electrodes were facing each other vertically at a distance of about 2 cm. A saturated (KCl) Ag/AgCl electrode was used as reference electrode.

2.2. Experimental conditions

The corrosion behavior of Al alloys AA6061 and AA5052 in 3.5% NaCl solution and when this solution is doped with each of acetate, chromate and citrate at 0.002 M have been studied by potentiodynamic polarization, EIS and EN techniques.

Table 3. Experimental conditions.

Run	Solution
Bln	NaCl 3.5%
Ace	NaCl 3.5% + Sodium acetate 0.002M
Chr	NaCl 3.5% + Sodium chromate 0.002M
Cit	NaCl 3.5% + Sodium citrate 0.002M

Table 3 provides the experimental conditions. Potentiodynamic polarization, EIS and EN experiments were conducted using an Autolab 302N potentiostat with Nova 1.6 software. This equipment allows resolutions of 0.76 μV for voltage signals and 10 nA for current signals. Potentiodynamic polarization and EIS measurements were conducted in a conventional three-electrode cell. A platinum rod was used as the counter and a saturated (KCl) Ag/AgCl electrode as reference electrode. The samples were immersed 1.5 h in the solution before EIS and potentiodynamic polarization measurements. Polarization curves were recorded at a scan rate of 1 mV/s and Nova software was used for determination of corrosion current densities. A sinusoidal potential perturbation of 10 mV versus OCP was used in the EIS measurements and a frequency range from 10 mHz to 100 kHz was employed.

The EN records were collected after 15 minutes from the immersion time and during 2 hours. All of the experiments were carried out at $25 \pm 1^0 C$ without passing any gas. Although EN studies tend to include both current and potential signals, this study concentrated on current signals only. The sampling frequency for the electrochemical noise data was 4Hz. The surfaces of alloy were observed in a CamScanMV2300 scanning electron microscope (SEM).

Noise data were analyzed with wavelet technique using the orthogonal Daubechies wavelets of the fourth order (db4). The necessary calculations for construction of the SDPS plots were performed using Matlab software.

3. RESULTS AND DISCUSSION

3.1 Potentiodynamic polarization

Fig. 1 shows the Tafel curves of AA6061 and AA5052 alloys in four Runs Bln, Ace, Chr and Cit. The relevant parameter values are listed in Table 4 (corrosion potential and corrosion current density). According to the values of corrosion current density (i_{corr}) of both AA6061 and AA5052 alloys it is clear that acetate and chromate act as corrosion inhibitors while citrate serves as corrosion accelerator.

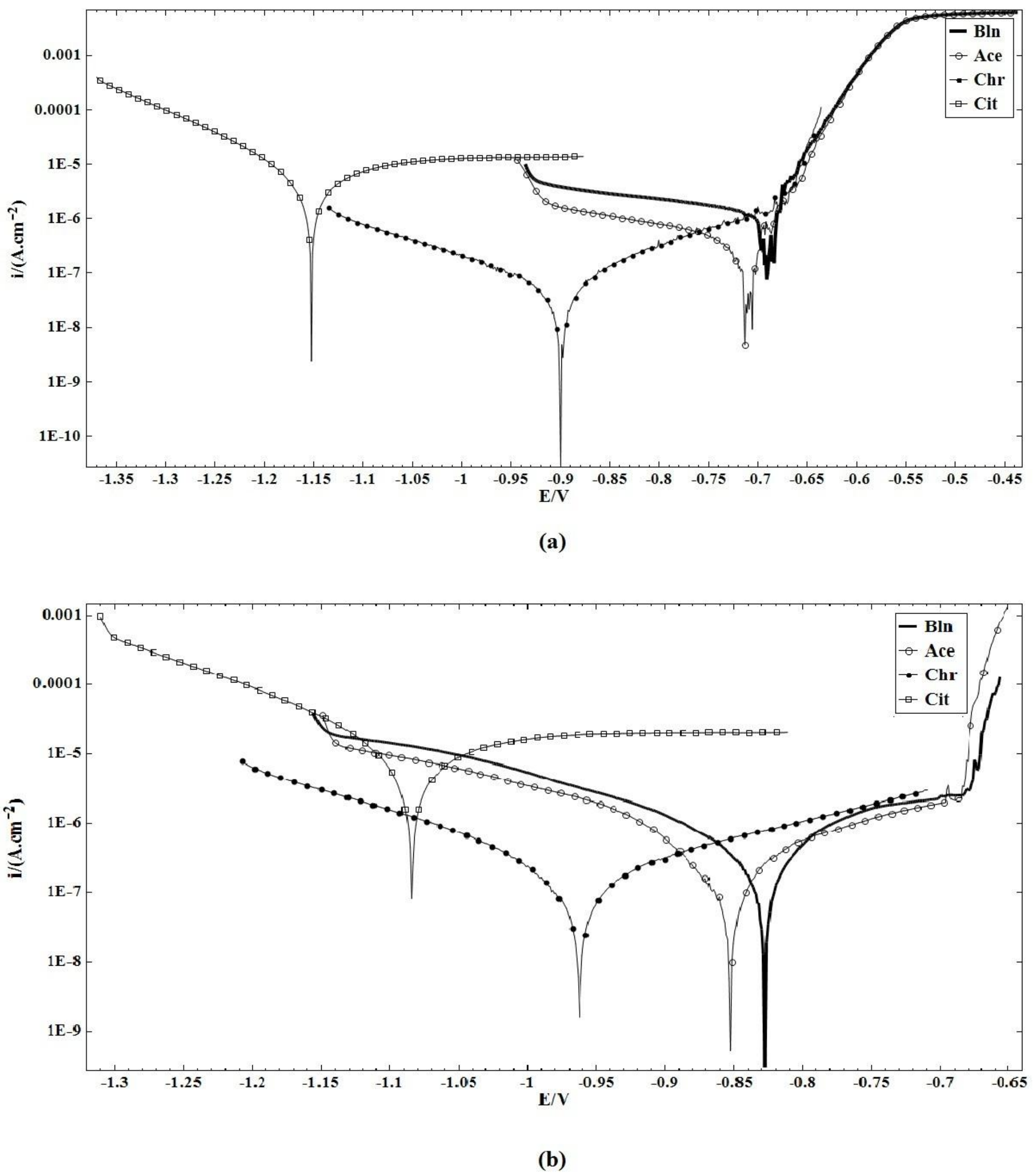

Figure 1. Potentiodynamic polarization curves of (a) AA6061 and (b) AA5052 in 3.5% NaCl solution (Bln) and doped solutions with each of acetate, chromate and citrate at 0.002 M.

Table 4. Potentiodynamic polarization parameter values for the corrosion of Al alloys in 3.5% NaCl without (Bln) and with different anions.

Run	AA6061			AA5052		
	$-E_{corr}$/mV	$i_{corr}/\mu A.cm^{-2}$	IE%	$-E_{corr}$/mV	$i_{corr}/\mu A.cm^{-2}$	IE%
Bln	690	1.27	-	828	0.932	-
Ace	714	0.482	62	853	0.520	44
Chr	900	0.068	95	963	0.092	90
Cit	1153	5.4	-	1085	6.77	-

Table 4 presents values of the corrosion inhibition efficiency (IE) of acetate and chromate for which the expression in this case is:

$$IE\% = \frac{i_{corr} - i'_{corr}}{i_{corr}} \times 100 \qquad (2)$$

where i_{corr} and i'_{corr} are corrosion current densities in the uninhibited and inhibited cases, respectively.

Belonging to carboxyl group, acetate is well capable of adsorbing on the metal surface and it can compete with the chloride ion leading to lesser corrosion activity. This process is reflected by the lower corrosion current density in Run Ace than in Run Bln (Table 4).

The role of chromate as a passivator for Al and its alloys can be explained by its powerful oxidizing properties and its adsorbability on the material surface [19]. The presence of chromate in the solution, even in the presence of aggressive anions like chloride, stimulates the repair of flawed regions of the surface film and oxidizes the active sites, leading to the formation of a stable corrosion resistant barrier film. Therefore, the corrosion current density is remarkably lower in Run Chr than in Run Bln (Table 4).

Citrate, similar to acetate, is a carboxylate anion and one may envisage that it can show the inhibition action on the Al alloys. But according to corrosion current density given in Table 4, citrate, unlike acetate, behaves as a corrosion accelerator. This is due to the complex formation between citrate anion as a tetradentate chelating agent and Al^{3+} cation (Fig. 2) [20].

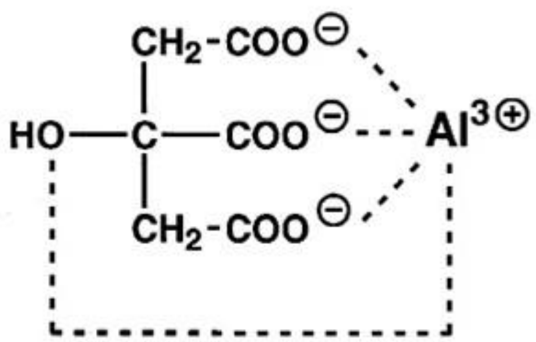

Figure 2. Simplified presentation of the complex formation between citrate anion and Al^{+3}.

Therefore, the presence of citrate in the solution causes the formation of AlCit complex and thereby decreasing the potential of Al alloy according to the following reactions:

$$Al \longrightarrow Al^{3+} + 3e^{-} \quad (3)$$

$$Al^{3+} + Cit^{3-} \longrightarrow AlCit \quad (4)$$

This is evident from the corrosion potentials (E_{corr}) in Table 4.

3.2 Electrochemical impedance spectroscopy

Bode plots of EIS for AA6061 and AA5052 in 3.5% NaCl in the absence and presence of various anions (acetate, chromate and citrate) are shown in Fig. 3. Table 5 lists impedance parameters in the absence and presence of different anions. These results prove the corrosion accelerating of citrate and the inhibition action of both acetate and chromate in agreement with the potentiodynamic polarization measurements.

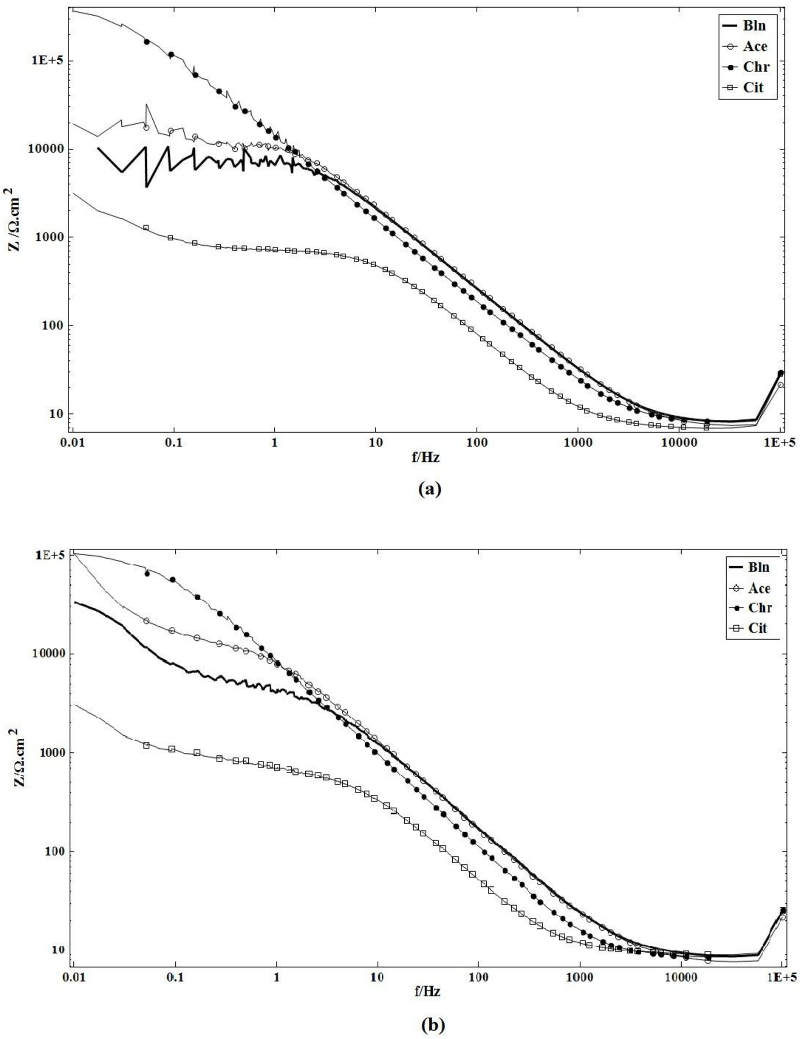

Figure 3. Bode plots of (a) AA6061 and (b) AA5052 exposed to 3.5% NaCl solution (Bln) and doped solutions with each of acetate, chromate and citrate at 0.002 M.

Table 5. Impedance parameter values for the corrosion of Al alloys in 3.5% NaCl without (Bln) and with different anions.

Run	**AA6061**		**AA5052**	
	R_{ct} (kΩ.cm^2)	IE%	R_{ct} (kΩ.cm^2)	IE%
Bln	7.2	-	9.2	-
Ace	15.4	53	16.8	45
Chr	361	98	98	91
Cit	0.77	-	0.85	-

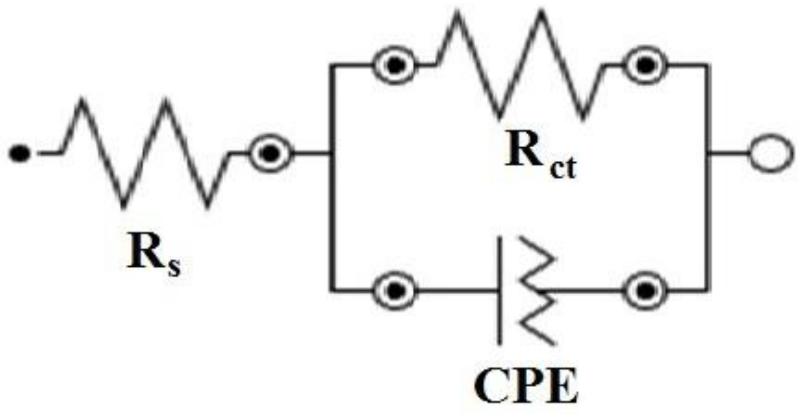

Figure 4. The equivalent electrical circuit of the impedance spectra.

Fig. 4 shows the electrical equivalent circuit employed to analyze the impedance plots. In this figure, R_s is the solution resistance and R_{ct} is the charge transfer resistance. Inhibition efficiencies in Table 5 were calculated through the following expression:

$$IE\% = \frac{R_{ct}^{'} - R_{ct}}{R_{ct}^{'}} \times 100 \qquad (5)$$

where R_{ct} and $R_{ct}^{'}$ represent the charge transfer resistance, before and after addition of the inhibitor to the corrosion media, respectively. Comparison with the data in Table 4 learns that satisfactory agreement is found with the inhibition efficiencies as obtained through potentiodynamic polarization measurements for acetate and chromate.

3.3 Electrochemical noise

Fig. 5 gives the current noise signals of four runs in Table 3 for AA6061 and AA5052 alloys taken during 2h of exposure. From a direct visual inspection of Fig. 5, it is clear that Signal Chr is a very low intensity and fast oscillating signal. Furthermore, current fluctuates very frequently in Signals Bln and Ace, but slowly in Signal Cit.

To characterize the current noise, EN time records are analyzed using wavelet transform. It has been found recently that a new kind of representation, SDPS plot, might improve the analysis of EN data and that has been used to characterize and distinguish time records [13]. Here to find the differences in corrosion behavior of the systems, the SDPS plots are employed. For this purpose WT was employed to decompose each set of 28800 data points and then the SDPS plots were obtained as shown in Figs. 6 and 7 for AA6061 and AA5052, respectively.

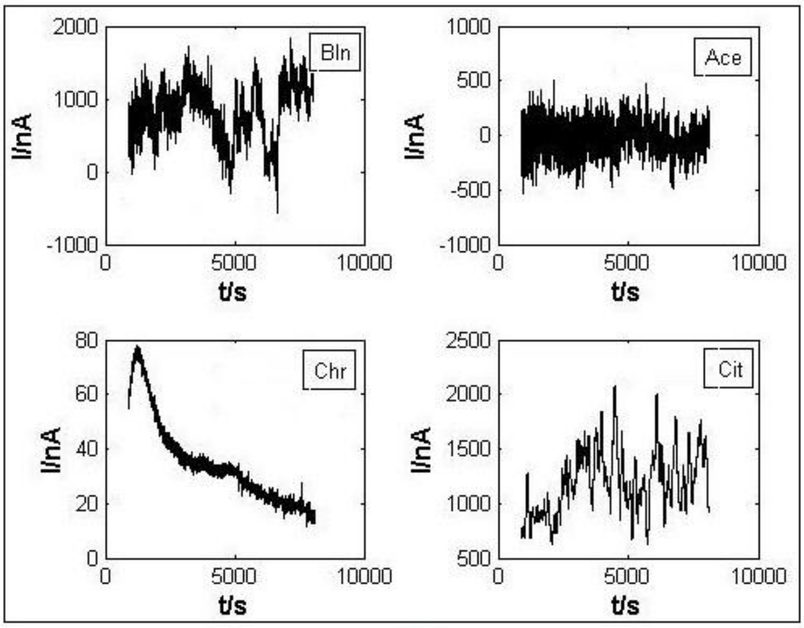

(a)

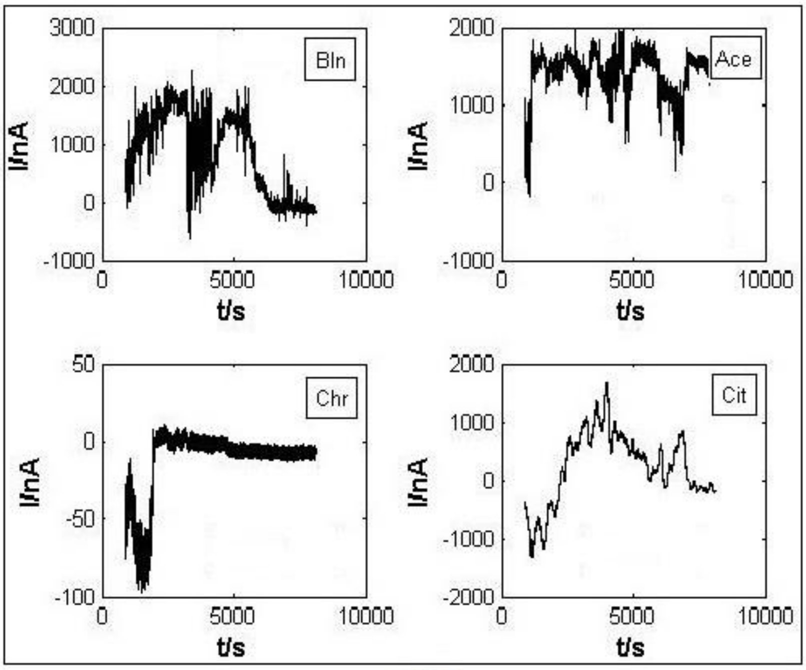

(b)

Figure 5. EN current records of (a) AA6061 and (b) AA5052 in 3.5% NaCl solution (Bln) and doped solutions with each of acetate, chromate and citrate at 0.002 M during 2 h after 15 min from the immersion time.

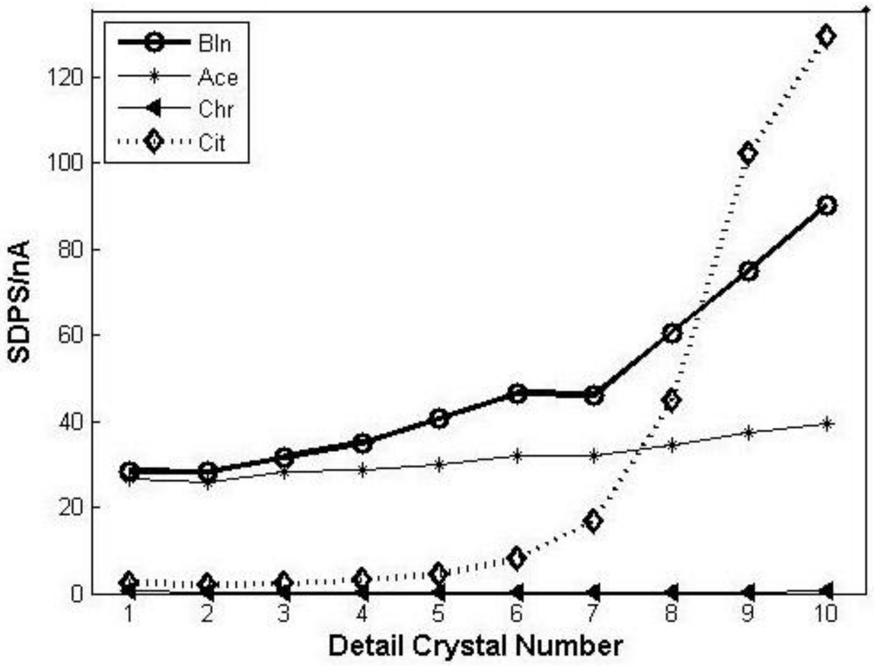

(a)

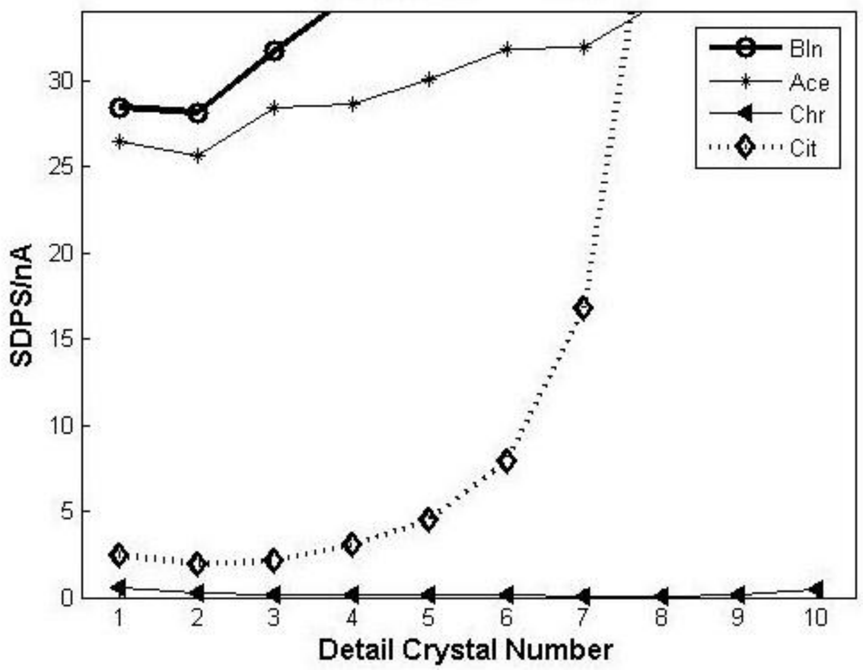

(b)

Figure 6. (a) SDPS plots of EN signals in Fig. 5a (b) the enlargement of SDPS plots of Signals Ace, Chr and Cit.

In general, the maximum peak in the SDPS plot corresponds to predominant transients in the original EN signal [13]. In the SDPS plots of AA6061 (Fig. 6) a maximum peak is defined at the position of d6 crystal for Signal Bln (Fig. 6a), d3 cyrstal for Signal Ace and d1 crystal for Signal Chr (Fig. 6b). The SDPS plot of Signal Cit doesn't show an apparent maximum peak. Comparison between partial and original signals provides an alternative way of recognizing the scale of the predominant transients [14]. Therefore, by using of partial signals it can be shown that the predominant transients of Signal Cit correspond to d6 crystal. Fig. 8 shows a part of the original Signal Cit with three predominant transients. These transients display a sudden increase followed by exponential decay, which is the characteristic of metastable pitting of Al [21].

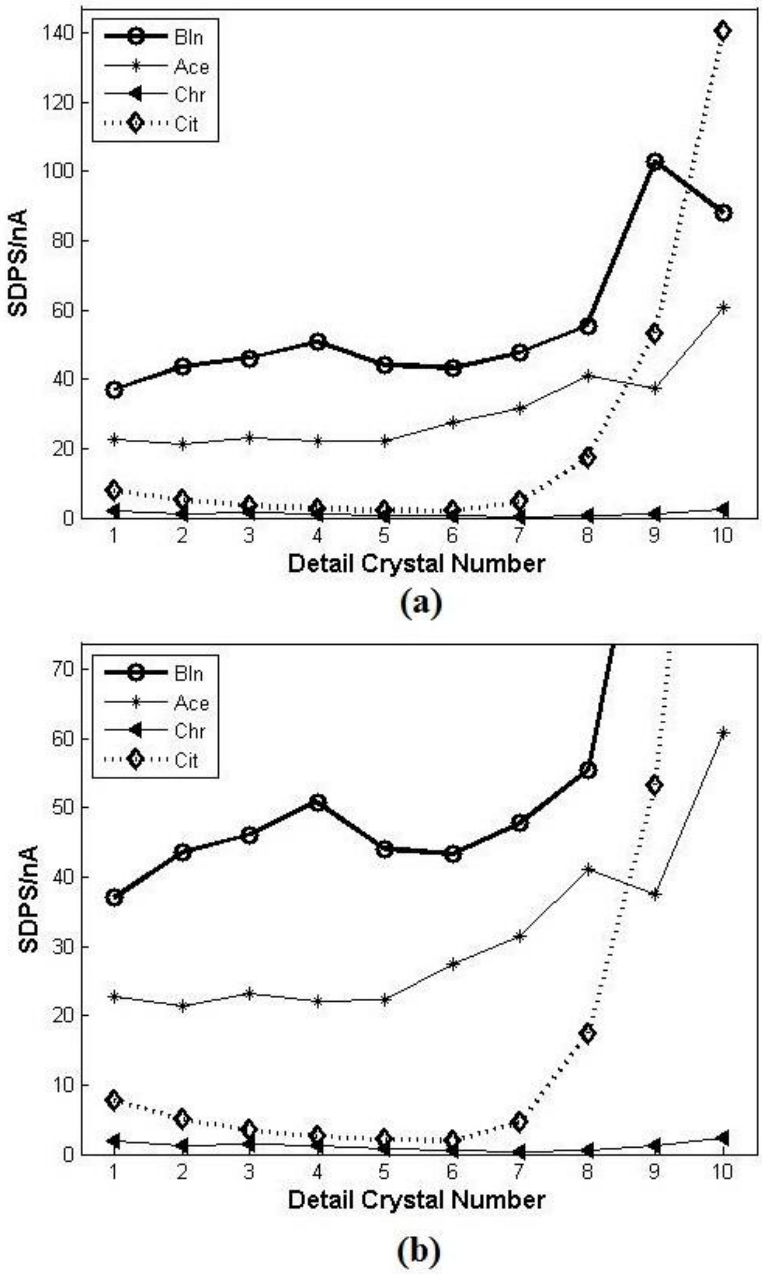

Figure 7. (a) SDPS plots of EN signals in Fig. 5b and (b) the enlargement of them.

The SDPS plots of AA5052 (Fig. 7) show a maximum peak at the position of d4 crystal for Signal Bln and d3 cyrstal for Signals Ace and Chr (Fig. 7b). Comparison between partial and original signals presents d6 crystal corresponding to the scale of the predominant transients in Signal Cit.

In general, the energy of current time records accumulates at crystals of shorter scale for the system with inhibitor than for the system without the inhibitor [7]. This means that the time width of predominant transients is shorter when solution contains inhibitor. The occurrence of the maximum peak of Signals Ace and Chr at lower crystals than that of Signal Bln proves the inhibition action of acetate and chromate on the corrosion of alloys. This suggests that Signals Ace and Chr are dominated by transients with a time width shorter than that underlying Signal Bln.

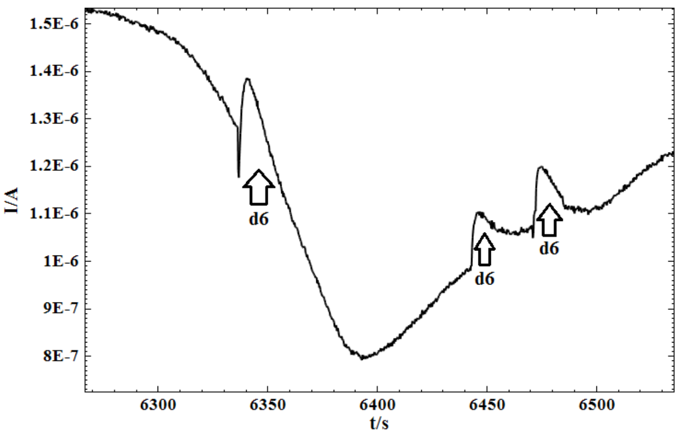

Figure 8. A part of the original signal of Signal Cit in Fig. 5a.

It is possible to categorize several corroding systems according to the pit size occurring on the surface of alloy using SDPS plots. The SDPS values at the maximum peak crystal can be treated similar to the calculations of the amount of charges contained in a current. The development of a pit causes a quantity of electric charge to flow in the circuit which can be estimated by the following equation:

$$q = i_p \times t_p \qquad (6)$$

where i_p is the SDPS value at the maximum peak crystal (d_p), t_p is the average time width of d_p crystal. Then q is a measure of the pit size taken place on the surface of alloy.

Table 6. Parameters in Eq. 6 for evaluation of the pit size on the Al alloys in 3.5% NaCl without (Bln) and with different anions.

Signal	AA6061				AA5052			
	d_p	t_p/s	i_p/nA	$10^9 q/C$	d_p	t_p/s	i_p/nA	$10^9 q/C$
Bln	d6	12	46.5	558	d4	3.0	50.8	152
Ace	d3	1.5	28.4	43	d3	1.5	23.3	35
Chr	d1	0.38	0.6	0.23	d3	1.5	1.5	2.2
Cit	d6	12	7.9	95	d6	12	2.0	24

Table 6 presents the values of these parameters obtained from EN signals of AA6061 and AA5052 alloys. Based on the data given in Table 6 it is possible to arrange the corroding solutions according to the pit size occurring on the surface as: Bln>>Cit>Ace>Chr for AA6061 and Bln>Ace>Cit>Chr for AA5052. These orders can be confirmed by SEM images in Figs. 9 and 10.

Table 7. Slope values of the SDPS plots after the maximum peak.

Signal	AA6061	AA5052
	Slope	Slope
Bln	14.6	11.6
Ace	1.8	5.7
Chr	0.0	0.03
Cit	39.5	44.3

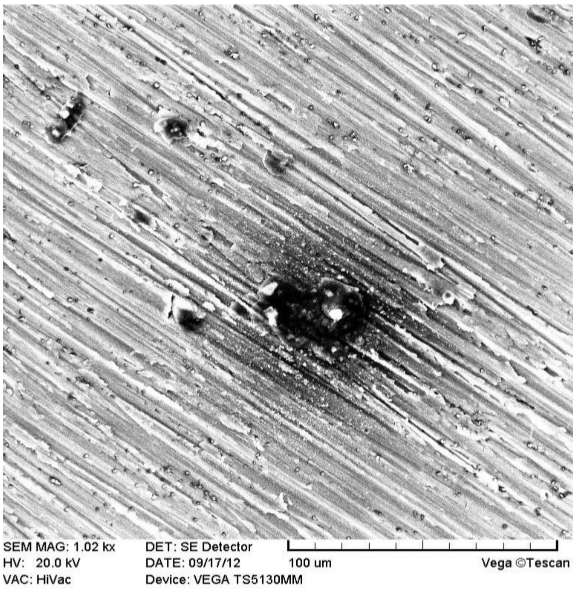

(a)

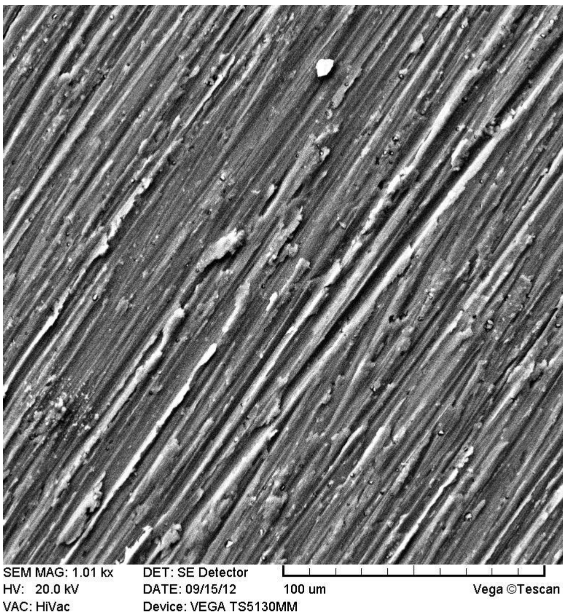

(b)

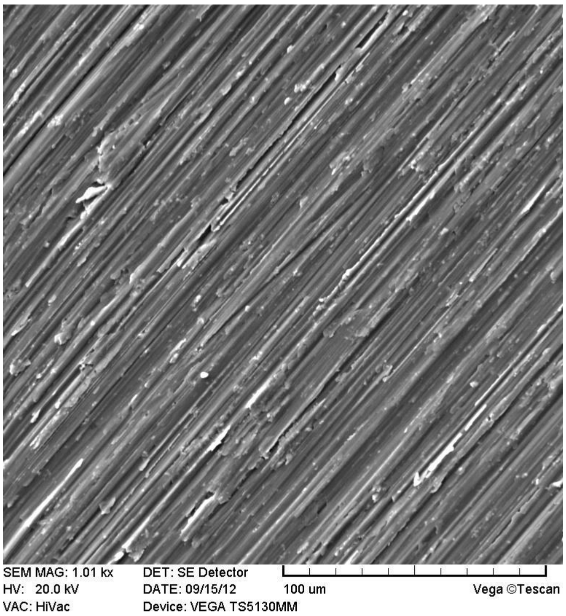

(c)

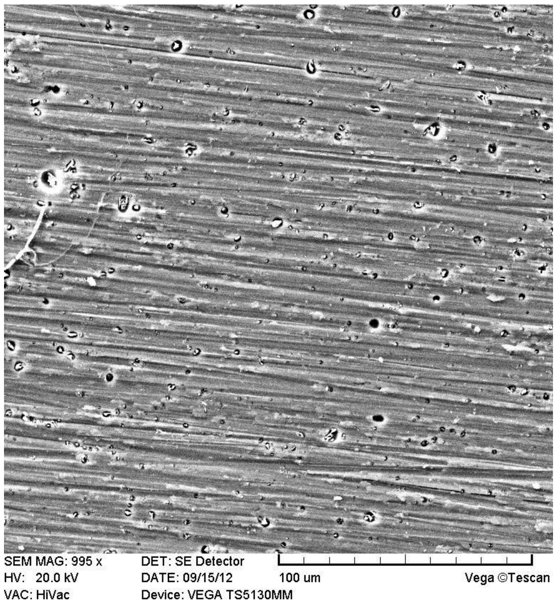

(d)

Figure 9. SEM images of AA6061 surface after EN experiments in Runs (a) Bln (b) Ace (c) Chr and (d) Cit.

In the presence of chromate, the breakdown probability of the oxide film decreases greatly in chloride media because chromate is an oxidizer and can reinforce the oxide film of the Al alloy surface. Thus, the pit size in Run Chr should be much lower than that in the other runs. Carboxylates in general provide an anion that could competitively adsorb on the surface of aluminum alloy instead of chloride ion to reduce the rupture probability of the oxide film [6]. This justifies the lower pit size in Runs Ace and Cit than that in Run Bln.

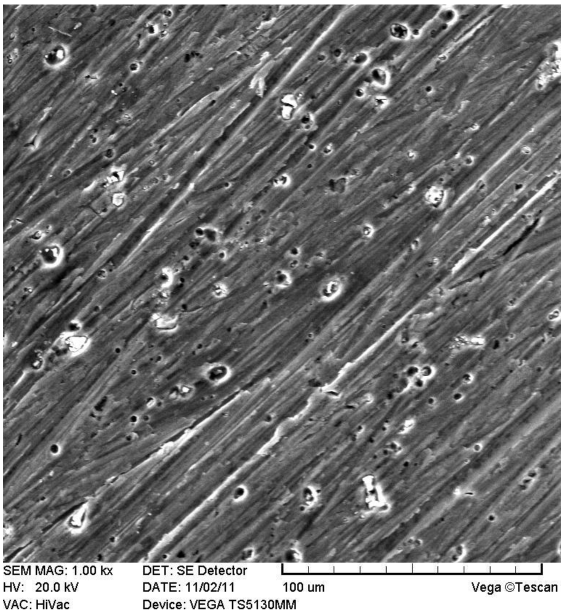
SEM MAG: 1.00 kx
DET: SE Detector
HV: 20.0 kV
DATE: 11/02/11
100 um
Vega ©Tescan
VAC: HiVac
Device: VEGA TS5130MM

(a)

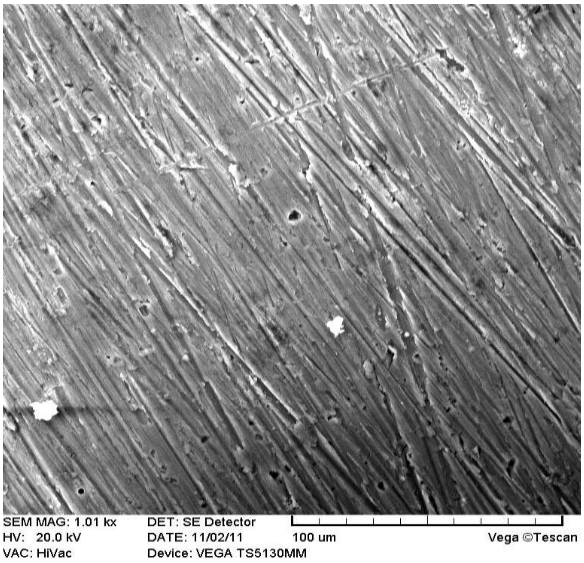
SEM MAG: 1.01 kx
DET: SE Detector
HV: 20.0 kV
DATE: 11/02/11
100 um
Vega ©Tescan
VAC: HiVac
Device: VEGA TS5130MM

(b)

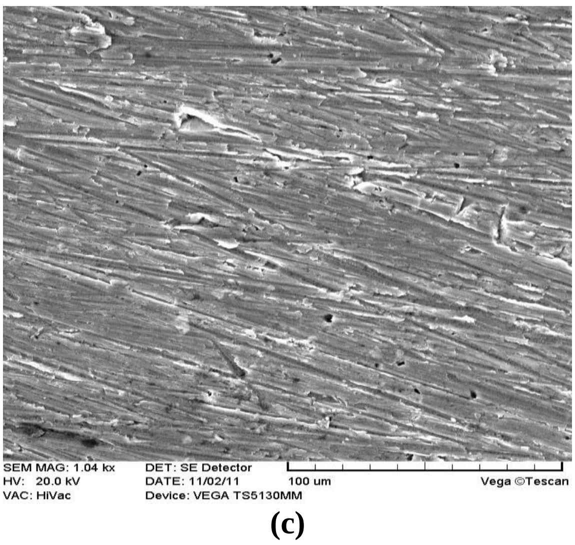
SEM MAG: 1.04 kx
DET: SE Detector
HV: 20.0 kV
DATE: 11/02/11
100 um
Vega ©Tescan
VAC: HiVac
Device: VEGA TS5130MM

(c)

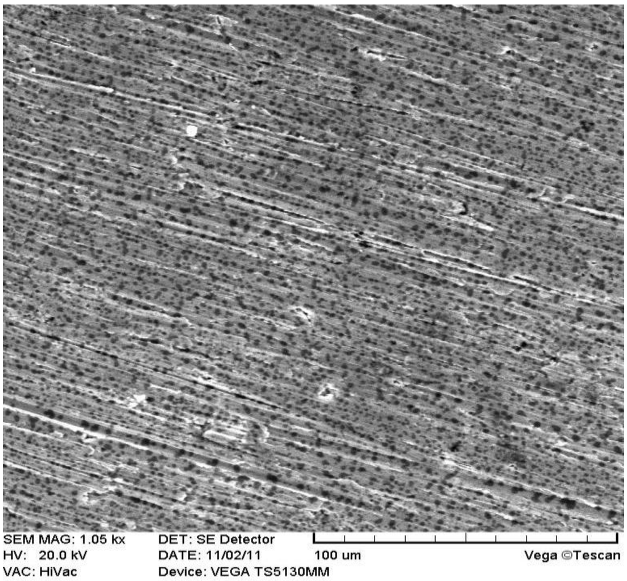

(d)

Figure 10. SEM images of AA5052 surface after EN experiments in Runs (a) Bln (b) Ace (c) Chr and (d) Cit.

Another aspect of interest of SDPS plots is the ability to classify several corroding systems according to the pit density based on the slope values of the SDPS plots in the region after the maximum peak [13]. Table 7 presents the slope values of the SDPS plots in Figs. 6 and 7 for AA6061 and AA5052 alloys. It is possible to arrange the corroding solutions according to the pit density occurring on the surface based on the slope values (Table 7) as: Cit>Bln>Ace>Chr for both AA6061 and AA5052. The SEM images in Figs. 9 and 10 verify these results.

The behavior of citrate is interesting. Based on the data in Table 6, it can be deduced that citrate acts as the pit size inhibitor due to a decrease in the pit size in Cit Run. On the other hand, according to the SDPS slopes (Table 7) it seems that citrate serves as the pit density accelerator. This dual action of citrate can be attributed to its combined action of a strongly adsorbed anion on the surface and a ligand to form a complex with Al^{+3}.

Table 8. Total amount of noise charges (Q) and inhibition efficiencies obtained from EN measurements.

Signal	AA6061		AA5052	
	$10^6 Q/C$	IE%	$10^6 Q/C$	IE%
Bln	22.5	-	19.5	-
Ace	10.3	54	12.3	37
Chr	0.1	99	0.3	98
Cit	28.7	-	23.0	-

As mentioned above in Section 1, each PS is a signal which resembles the fluctuations of the original signal at a particular frequency interval. Therefore, it is suitable to use the absolute mean of partial signal (AMPS) for calculation of the amount of noise charges at the particular frequency interval. After calculation of the mean time width of each crystal, the amount of noise charges due to the ith PS, Q_i, can be computed. The Q_i values can be summed to give the total amount of noise charges, Q. Table 8 shows Q values for AA6061 and AA5052 alloys in different solutions.

It seems suitable to define the corrosion inhibition efficiency as follows:

$$IE\% = \frac{Q - Q'}{Q} \times 100 \qquad (7)$$

where Q and Q' are the noise charges in the uninhibited and inhibited cases, respectively. Table 8 presents IE values obtained with EN measurements on AA6061 and AA5052 in the presence of acetate and chromate inhibitors. Comparison with data in Tables 4 and 5 reveals that the reasonable agreement is found with the IE values as obtained through potentiodynamic polarization and EIS measurements.

4. CONCLUSIONS

The objective of this paper is to compare the results obtained from polarization and EIS techniques with those acquired from the wavelet analysis of EN measurements on the pitting corrosion of Al alloys. The wavelet analysis of EN data can be applied as an alternative technique to study the pitting corrosion behavior of Al alloys. The study of the SDPS plots provides a convenient way of comparing both the pit size and pit density in several corroding systems.

The SDPS plots prove the inhibition action of acetate and chromate both on the pit size and the pit density of Al alloys. According to the SDPS plots it is recognized that citrate shows the inhibition effect on the pit size and the acceleration effect on the pit density. In addition, according to calculation of the total amount of noise charges arising from all of PSs it is possible to obtain the inhibition efficiency of an inhibitor. The inhibition efficiencies show a reasonable agreement with those obtained from potentiodynamic polarization and EIS. Thus, the wavelet analysis of EN data seems as an alternative tool to overcome the limitations of the potentiodynamic polarization and EIS techniques in the pitting corrosion monitoring applications.

ACKNOWLEDGEMENTS
This work has received financial support from Islamic Azad University, Kerman Branch.

References

1. R.A. Cottis, *Corrosion*, 57 (2001) 265.
2. K.-H. Na and S.-I. Pyun, *J. Electroanal. Chem.*, 596 (2006) 7.
3. A. Aballe, M. Bethencourt, F.J. Botana and M. Marcos, *Electrochim. Acta*, 44 (1999) 4805.
4. A. Aballe, M. Bethencourt, F.J. Botana and M. Marcos, *Electrochem. Commun.* , 1 (1999) 266.
5. A. Aballe, M. Bethencourt, F.J. Botana, M. Marcos and J.M. Sanchez-Amaya, *Electrochim. Acta*, 46 (2001) 2353.
6. X.F. Liu, H.G. Wang, S.J. Huang and H.C. Gu, *Corrosion*, 57 (2001) 843.

7. A. Aballe, M. Bethencourt, F.J. Botana, M. Marcos and R.M. Osuna, *Electrochim. Acta*, 47 (2002) 1415.
8. J.A. Wharton, R.J.K. Wood and B.G. Mellor, *Corros. Sci.*, 45 (2003) 97.
9. C. Cai, Z. Zhang, F. Cao, Z. Gao, J. Zhang and C. Cao, *J. Electroanal. Chem.*, 578 (2005) 143.
10. X.F. Liu, H.G. Wang and H.C. Gu, *Corros. Sci.*, 48 (2006) 1337.
11. M. Shahidi, R.Farrehi Moghaddam, M.R. Gholamhosseinzadeh and S.M.A. Hosseini, J. Electroanal. Chem., 693 (2013) 114.
12. M.T. Smith and D.D. Macdonald, *Corrosion*, 65 (2009) 438.
13. M. Shahidi, S.M.A. Hosseini and A.H. Jafari, *Electrochim. Acta*, 56 (2011) 9986.
14. M. Shahidi, A.H. Jafari and S.M.A. Hosseini, *Corrosion*, 68 (2012) 1003.
15. X. Wang, J. Wang, C. Fu and Y. Gao, *Int. J. Electrochem. Sci.*, 8 (2013) 7211.
16. W.J. Rudd and J.C. Scully, *Corros. Sci.*, 20 (1980) 611.
17. A.K. Maayta and N.A.F. Al-Rawashdeh, *Corros. Sci.*, 46 (2004) 1129.
18. R. Rosliza, A. Nora'aini and W.B.W. Nik, *J. Appl. Electrochem.*, 40 (2010) 833.
19. W.A. Badawy, F.M. Al-Kharafi and A.S. El-Azab, *Corros. Sci.*, 41 (1999) 709.
20. B. Muller, *Corros. Sci.*, 46 (2004) 159.
21. J. Soltis, D.P. Krouse, N.J. Laycock and K.R. Zavadil, *Corros. Sci.*, 52 (2010) 838.